SERI/TR-254-3356
UC Category: 232
DE89000815

Short-Term Energy Monitoring (STEM):

Application of the PSTAR Method to a Residence in Fredericksburg, Virginia

K. Subbarao
J.D. Burch
C.E. Hancock
A. Lekov
J.D. Balcomb

September 1988

Prepared under Task No. SB811241

Solar Energy Research Institute
A Division of Midwest Research Institute

1617 Cole Boulevard
Golden, Colorado 80401-3393

Prepared for the
U.S. Department of Energy
Contract No. DE-AC02-83CH10093

Printed in the United States of America
Available from:
National Technical Information Service
U.S. Department of Commerce
5285 Port Royal Road
Springfield, VA 22161

Price: Microfiche A01
Printed Copy A03

Codes are used for pricing all publications. The code is determined by the number of pages in the publication. Information pertaining to the pricing codes can be found in the current issue of the following publications, which are generally available in most libraries: *Energy Research Abstracts, (ERA); Government Reports Announcements* and Index (*GRA* and I); *Scientific and Technical Abstract Reports (STAR);* and publication, NTIS-PR-360 available from NTIS at the above address.

PREFACE

In keeping with the national energy policy goal of fostering an adequate supply of energy at a reasonable cost, the United States Department of Energy (DOE) supports a variety of programs to promote a balanced and mixed energy resource system. The mission of the DOE Solar Buildings Research and Development Program is to support this goal by providing for the development of solar technology alternatives for the buildings sector. It is the goal of the program to establish a proven technology base to allow industry to develop solar products and designs for buildings that are economically competitive and can contribute significantly to the nation's building energy supplies. Toward this end, the program sponsors research activities related to increasing the efficiency, reducing the cost, and improving the long-term durability of passive and active solar systems for building water and space heating, cooling, and daylighting applications. These activities are conducted in four major areas: Advanced Passive Solar Materials Research, Collector Technology Research, Cooling Systems Research, and Systems Analysis and Applications Research.

Advanced Passive Solar Materials Research - This activity area includes work on new aperture materials for controlling solar heat gains, and for enhancing the use of daylight for building interior lighting purposes. It also encompasses work on low-cost thermal storage materials that have high thermal storage capacity and can be integrated with conventional building elements, and work on materials and methods to transport thermal energy efficiently between any building exterior surface and the building interior by nonmechanical means.

Collector Technology Research - This activity area encompasses work on advanced low- to medium-temperature (up to 180°F useful operating temperature) flat-plate collectors for water and space heating applications, and medium- to high-temperature (up to 400°F useful operating temperature) evacuated tube/concentrating collectors for space heating and cooling applications. The focus is on design innovations using new materials and fabrication techniques.

Cooling Systems Research - This activity area involves research on high-performance dehumidifiers and chillers that can operate efficiently with the variable thermal outputs and delivery temperatures associated with solar collectors. It also includes work on advanced passive cooling techniques.

Systems Analysis and Applications Research - This activity area encompasses experimental testing, analysis, and evaluation of solar heating, cooling, and daylighting systems for residential and nonresidential buildings. This involves system integration studies, the development of design and analysis tools, and the establishment of overall cost, performance, and durability targets for various technology or system options.

The research described in this report was supported by the Office of Solar Heat Technologies. It was performed as part of the Short-Term Energy Monitoring (STEM) project. The goal of the project is to develop, field test, and transfer to industry a technique for assessing the energy performance of a residential building through short-term tests. Extensions to nonresidential buildings, especially for control and diagnostics of heating, ventilation, and air-conditioning systems are planned for the future.

Larry Palmiter of Ecotope made the modifications to the SUNCODE-PC program. Don Carr of Legacy Homes made available the building for tests.

The authors gratefully acknowledge useful discussions with C. B. Christensen, and L. Palmiter.

Kris Subbarao, Senior Physicist

Approved for

SOLAR ENERGY RESEARCH INSTITUTE

Terry R. Penney, Manager
Buildings Research Branch

Robert A. Stokes, Acting Director
Solar Heat Research Division

ABSTRACT

This report describes a project to assess the thermal quality of a residential building based on short-term tests during which a small number of data channels are measured. This project is called Short-Term Energy Monitoring (STEM). Setting up the instrumentation to measure a small number of data channels (approximately 20) typically takes less than a half-day's labor. The tests last a few days. Analysis of the data provides extrapolation to long-term performance.

The test protocol and analysis are based on a unified method for building simulations and short-term testing, called Primary and Secondary Terms Analysis and Renormalization (PSTAR). The mathematical formulation of PSTAR is detailed in earlier reports. This report describes the short-term tests and data analysis performed using the PSTAR method on a residential building in Fredericksburg, Virginia.

The PSTAR method starts with a building description obtained from a site visit ("audit"). The energy balance is decomposed into a number of terms: static losses, charging and discharging of masses from variations in indoor and outdoor temperatures, solar gains, infiltration, and heat flow caused by sky temperature depression, etc. Each term is obtained from a calculation given the weather and the building description. (Some heat flows, such as electric heat input, are directly measured.) Because the calculations are done from the audit description, which is usually different from the as built, the energy balance equation is not satisfied. The heat flow terms are now classified as either primary or secondary, depending on their overall magnitude. The primary terms are renormalized using a linear least squares fit. (Hence, the name PSTAR.) The resulting renormalized energy balance equation allows an hour-by-hour simulation of the as-built building. Extrapolation to long-term performance and building-as-a-calorimeter measurements are now possible.

The results demonstrate the ability of the PSTAR method to provide a realistically complex thermal model of a building, and determine from short-term tests the statics as well as the dynamics of a building, including solar dynamics. Plots of the various heat flow terms provide valuable intuitive, as well as quantitative, information about building performance. Extrapolation to long-term performance and determination of peak loads has been explicitly demonstrated. The importance of a measurement-based evaluation of building performance can be seen from these results. Other important applications employing the building-as-a-calorimeter, such as heating, ventilating, and air conditioning system control and diagnostics, are pointed out.

TABLE OF CONTENTS

		Page
1.0	Introduction	1
2.0	Outline of the Method	3
	2.1 Steps in PSTAR	3
3.0	Building Description and the Data Acquisition System	5
	3.1 Building Description	5
	3.2 Data Acquisition System	5
4.0	Steps for the Building Under Study	9
	4.1 Step 1: Heat Flow Terms	9
	4.2 Step 2: Audit Description	11
	4.3 Step 3: Test Protocol	11
	4.4 Step 4: Test Data	13
	4.5 Step 5: Calculation of Heat Flows	15
	4.6 Step 6: Renormalization of Heat Flows	21
	4.6.1 Inclusion of Solar Transfer Function	23
	4.6.2 Simplified Renormalization	24
	4.7 Step 7: Long-term Extrapolation	26
5.0	Discussion	28
6.0	Summary and Conclusions	30
7.0	References	31
	Appendix	32

LIST OF FIGURES

Page

3-1 View of the building from the northwest..... 6

3-2 View of the building from the southeast..... 6

3-3 Floor plans for the building..... 7

4-1 Hourly averages of indoor temperatures at several locations during the short-term tests held March 15-17, 1988..... 14

4-2 Hourly averages of outdoor, crawl space and garage temperatures during the short-term tests..... 14

4-3 Hourly averages of solar irradiance on a horizontal pyranometer as well as that on a vertical pyranometer mounted parallel to the house in the westerly direction..... 15

4-4 Hourly averages of power in the six circuits individually monitored..... 16

4-5 Polar diagram (imaginary vs. real part) of the V-admittance (i.e., admittance with respect to indoor temperature)..... 16

4-6 Plot of four of the heat flow terms: $[-0.668(L+L_{inf}^{ch})\cdot(T_{in}(n) - T_{out}(n))]$, $[-L_b\ (T_{in}(n) - T_{bsm}(n))]$, $0.948\ Q_{storage}^{in}(n)$, and $Q_{storage}^{out}(n)$ 17

4-7 Plot of three of the heat flow terms: $0.895\ Q_{sun}(n)$, $0.106\ Q_{sun}^{shift}(n)$, and $[Q_{infil}(n) + L_{inf}^{ch}\cdot(T_{in}(n) - T_{out}(n))]$..... 19

4-8 Plot of three of the heat flow terms: $Q_{int}(n)$, $Q_{sky}(n)$, and $Q_{init}(n)$..... 21

4-9 Plot of the measured indoor temperature, predicted by the audit (unrenormalized) energy balance equation, and predicted by the renormalized energy balance equation..... 25

LIST OF TABLES

Page

3-1 Measurement Channels..... 8

4-1 Goodness of Least Squares Fit for Different Values of α_{sun}..... 24

1.0 INTRODUCTION

Thermal evaluation of a building is important for a number of purposes. Utility bill analysis is attractive from the viewpoint of simplicity and cost, but it has drawbacks, such as unknown occupancy effects, variations in weather (not all of which are easy to correct), and the length of time needed to obtain the necessary data. In addition, cause and effect relationships are not delineated. Reliance on a simulation based on nominal inputs results in significant uncertainties in the performance of the as-built building. A method is needed that takes short-term data on a small number of data channels, from which long-term performance is extrapolated.

A method meeting the above objective was developed for residential buildings under a project called Short-Term Energy Monitoring (STEM). By performing short-term tests on a building, the thermal parameters of a building can be obtained; these parameters lead to long-term extrapolation. Setting up the instrumentation to measure a small number of data channels (about 20) typically takes less than half a workday. The tests last a few days. Analysis of the data provides extrapolation to long-term performance as well as important building parameters.

The theoretical framework for defining the building parameters, test protocol, and data analysis is given by Primary and Secondary Terms Analysis and Renormalization (PSTAR), Subbarao (1988a). References to earlier literature are cited here. A summary of the PSTAR method is given in Subbarao (1988b). The purpose of this report is to explain the PSTAR method in the context of tests on a real building. Results from tests and analysis of a residential building (to be referred to as the "Fredericksburg house") in Fredericksburg, Virginia are given.

Short-term tests were conducted over a period of a few days following a certain test protocol. The test data were used to obtain the building loss coefficient, charging and discharging of the masses by variations in indoor temperatures as well as outdoor temperatures, solar gains with the appropriate phase lags, infiltration heat flows, and heat flows from sky temperature depression. The characteristics obtained from the short-term tests were then used for long-term extrapolation to obtain annual heating and cooling loads, as well as peak loads with and without thermostat setback.

The results demonstrate the ability of the PSTAR method to provide a realistically complex thermal model of a building, and determine from short-term tests the statics as well as the dynamics of a building, including solar dynamics. Although this leads to a number of applications, extrapolation to long-term performance was explicitly demonstrated. Some of the limitations of the study of this building as well as further work are cited in (Section 5.0).

Brief explanations for the application to the building under study are given as needed. For a detailed development of the method, consult the previously mentioned references. A Field User's Guide for PSTAR is planned.

Several buildings were tested and testing of more buildings is planned. Brief reports are being prepared on each building. This article covers details not present in the brief reports.

The thermal parameters obtained from the tests are useful for long-term extrapolation, predictive load control for demand reduction, building-as-a-calorimeter for heating, ventilating, and air conditioning (HVAC) diagnostics, and design versus actual parameter comparisons.

2.0 OUTLINE OF THE METHOD

Any short-term test method should specify the data channels, test protocol, and one-time measurements, as well as the analysis procedures.

The PSTAR method starts with an energy balance equation for each of the principal zones written with some mild assumptions in terms of a number of suitably disaggregated flows. Each of these terms is calculated from a quick audit description of the building, one-time measurements, and hourly data acquired during the test period following a certain test protocol. The necessary one-time tests, the data channels, and the test protocol can all be deduced from the energy balance equation. In general, the various heat flows will not satisfy the heat balance equation because the audit description is usually not an accurate description of the building. The various heat flow terms are renormalized using linear least squares to give a best fit. The resulting renormalized energy balance equation is used in the applications.

The unique feature of using an audit description results in a realistically complex model without too many parameters to be determined from performance data.

We can think of three descriptions of the building being monitored – "audit," "renormalized," and "as-built." A good microdynamic simulator and an as-built microlevel description of the building will answer all thermal questions, including long-term performance. Even though good microdynamic simulators (DOE-2, BLAST, etc.) may be available, an as-built microlevel description is rarely available. Is the audit microlevel description close enough to the as-built microlevel description? It usually is not, and this is one of the reasons for monitoring the building. Starting with an audit description and monitored data, we wish to get close to an as-built macrolevel description. (It is fruitless to try to get close to an as-built microlevel description.) The mathematical process for accomplishing this is to modify the audit energy balance equation into the renormalized energy balance equation. The renormalized energy balance equation is presumably close to the as-built energy balance equation. We will sometimes loosely refer to the renormalized building as the as-built building.

2.1 Steps in PSTAR

The various steps in the PSTAR process are:

1. Identify all the relevant heat flows for the building. Determine which of the three categories each term belongs: measured (such as electrical heat input), primary (such as the loss coefficient times the inside-outside temperature difference), or secondary (such as the flow due to sky temperature depression). How this determination is made is detailed later.
2. Obtain the audit description needed to calculate the flows.
3. Determine a test protocol to elicit the renormalization parameters.
4. Obtain test data.
5. Calculate the heat flows for the test period.

6. Obtain the renormalization parameters from linear least squares.
7. Use the renormalized energy balance equation for the intended application.

These steps for the Fredericksburg house are given in Section 4.0.

3.0 BUILDING DESCRIPTION AND THE DATA ACQUISITION SYSTEM

3.1 Building Description

The Fredericksburg house, located in Fredericksburg, Virginia, is a newly completed house built by Don Carr of Legacy Homes. The house is located at approximately 38.3N latitude, 77.5W longitude (about 50 miles southwest of Washington, D.C.). Site elevation is about 150 ft. It is located in an area with low-density detached housing.

The two-story house has approximately 2600 ft^2 of living area and an attached two-car garage. A view of the house from the northwest is given in Figure 3-1 and from the southeast in Figure 3-2. A floor plan is given in Figure 3-3. The house uses typical lightweight frame construction. Vertical walls are framed with 2 in. × 4 in. studs, 16 in. on center, with R-13 batts plus 0.5-in. polystyrene exterior sheathing. There is a vaulted ceiling (R-19) above the living room, dining room, and master bedroom. The remaining areas have horizontal ceilings with R-30 blown-in fiberglass insulation. The floor is insulated from the crawl space with R-19 fiberglass batts. All windows are double glazed with a 0.25 in. gap. The house was unoccupied during the tests and was unfurnished.

The long axis of the house runs north-south, making the dominant glazing orientations east (165 ft^2) and west (100 ft^2). The south and north orientations have 18 ft^2 and 27 ft^2 of glazing, respectively. The trees on the east and south sides provide significant shading.

Space heating and cooling is provided by a York 3.5-ton heat pump, with electric resistance backup. The heat pump indoor unit is located in the garage. There are about 6 ft of insulated duct in the garage. Air ducts run between the first and second floors. It was noted during the blower door tests that significant airflow occurred through the air handler registers.

3.2 Data Acquisition System

A data acquisition system was temporarily installed in the house. The commercially available data logger (from Fowlkes Engineering) is a lap-top computer with a 12-bit analog to digital converter. Data channels are scanned once every 10 sec, and hourly averages are stored in memory and transferred via modem link to a off-site microcomputer for analysis. Table 3-1 lists the data channels monitored.

Figure 3-1. View of the building from the northwest

Figure 3-2. View of the building from the southeast

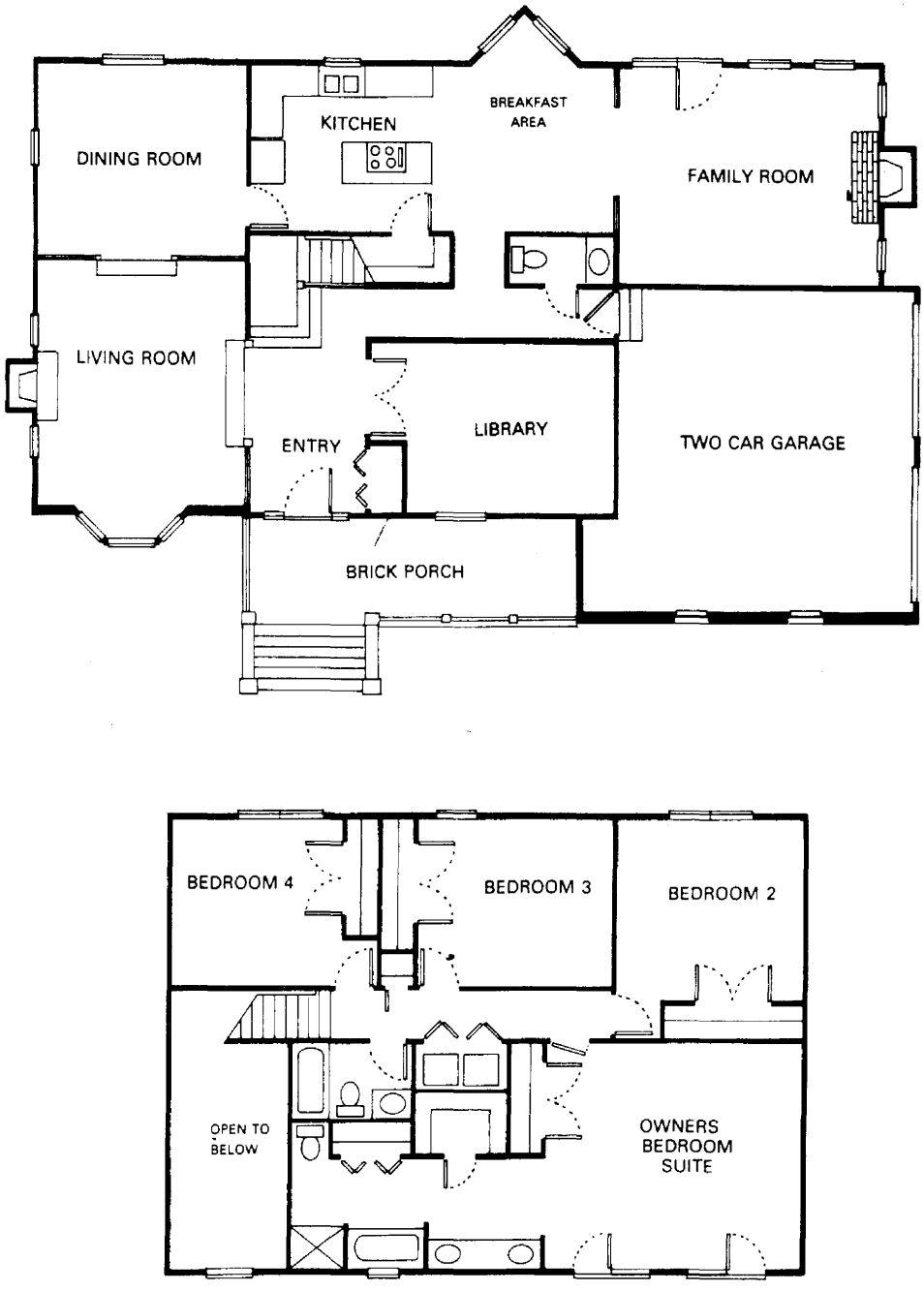

Figure 3-3. Floor plans for the building. The ground floor is shown at the top and the second floor at the bottom. The ground floor is over a partial crawl space. There is an attic over the three west bedrooms.

Table 3-1. Measurement Channels

	Quantity Measured	Sensor	Accuracy
1.	Solar Irradiance a. global horizontal b. west vertical	Li-Cor: Silicon PV	8%
2.	Electric Power (six circuits)	Ohio Semitronics Inc., Watt Transducer	1%
3.	Total House Power Two phases	Amp Clamp	5%
4.	Indoor Temperature - family room - living room - north bedroom - master bedroom	AD590, Semiconductor	0.8°F
5.	Outside Air Temperature	AD590, Semiconductor	1°F
6.	Crawl Space Temperature	AD590, Semiconductor	0.8°F
7.	Garage Temperatures	AD590, Semiconductor	0.8°F
8.	Wind Speed	Three Cup Anemometer	1%
9.	Relative Humidity		

4.0 STEPS FOR THE BUILDING UNDER STUDY

4.1 Step 1: Heat Flow Terms

We will now write the energy balance equation. The living areas in the two levels will be treated as one zone, while the crawl space will be treated as a separate zone. Because the crawl space is handled in much the same manner as a basement, we will use the subscript "b" or "bsm" for quantities referring to the crawl space. We will write the energy balance of the living zone. (Note the convention: all terms are written with a positive sign. Thus, positive values of any term imply a heat gain and negative values imply a heat loss from the indoor air node.)

$$
\begin{aligned}
& Q_{int}(n) \\
+ \; & [-L\,(T_{in}(n) - T_{out}(n))] \\
+ \; & [-L_b\,(T_{in}(n) - T_{bsm}(n))] \\
+ \; & Q^{in}_{storage}(n) \\
+ \; & Q^{out}_{storage}(n) \\
+ \; & Q_{bsm,\,storage}(n) \\
+ \; & Q_{sun}(n) \\
+ \; & Q_{infil}(n) \\
+ \; & Q_{sky}(n) \\
+ \; & Q_{aux}(n) = 0 \,, \qquad (4\text{-}1)
\end{aligned}
$$

where

Q_{int} are the internal gains. During short-term testing in an unoccupied building, it consists of electrical heat introduced through computer-controlled heaters to follow a specific profile. This is a measured term.

L is the steady-state loss coefficient. The second term is, therefore, the static heat loss caused by a difference between the inside temperature, T_{in}, and outside temperature, T_{out}. This is typically a primary term.

L_b is the conductance between the living zone and the crawl space. The second term is the static heat loss caused by the difference between the inside temperature and the crawl space temperature T_{bsm}. This term is tentatively determined to be a secondary term.

$Q^{in}_{storage}$ is the heat that goes to charge (discharge, if the term is negative) the mass in the building. This term is obtained from a building description and the T_{in} time series only. This term provides a correction to the first two terms resulting from dynamics. This is typically a primary term.

$Q^{out}_{storage}$ is the storage effect caused by mass coupled with T_{out}. This term is obtained from a building description and the T_{out} time series only. This term provides a correction to the first term resulting from dynamics. This is typically a secondary term.

$Q_{bsm,\ storage}$ is the storage effect caused by mass coupled to T_{bsm}. However, because the floor is lightweight and the crawl space temperature does not vary much, this term can be safely neglected. (Remember that we are concerned with energy balance of the main zone. Only the mass in the floor between the main zone and the basement is relevant for this purpose.)

Q_{sun} is the heat gain at the air node caused by solar radiation. This term is obtained by performing a simulation of the audit building with $T_{in} = T_{out}$ = constant (and with all other heat flows set to zero). The resulting cooling load gives Q_{sun}. This is typically a primary term (even for a "nonsolar" building, such as the one under consideration).

Q_{infil} is the heat loss caused by infiltration; this is obtained by a combination of one-time measurements and modeling. This flow requires further considerations; tentatively, we will treat this as a measured term.

Q_{sky} is the heat loss caused by sky temperature depression below ambient air temperature. This term is obtained through a simulation with $-h_{sky}(T_{out} - T_{sky})$ as a negative solar flux on the relevant surfaces (h_{sky} is the radiative conductance to the sky and T_{sky} the effective sky temperature for the given surface). This is typically a secondary term.

Q_{aux} is the heating energy supplied by the heating system. This flow is typically a primary term. A separate report will give the results from tests involving the heating system. For the purposes of the present report, analysis is done only of data from tests when this term is zero.

In Eq. 4-1, we can add a quantity to one term and subtract it from another. For reasons given later, let us add a constant times $T_{in} - T_{out}$ to Q_{infil} and subtract it from the second term. We will choose the constant to be the average value of the infiltration loss coefficient during a part of the test period (this part is the coheating period described later); this constant will be denoted L^{ch}_{inf}.

The initial state of the building is unknown. The corresponding heat flow decays exponentially. After a sufficiently long time (about 6 hours for conventional residential buildings), this flow can be neglected. An alternative is to introduce suitable parameters to represent the initial state and estimate them. Even though the former is recommended in a simplified procedure, we will first illustrate the latter. A heat flow term $Q_{init}(n)$ is needed in the energy balance equation to represent the initial state.

Because the audit description generally deviates from the as-built, the energy balance equation will not be obeyed. We introduce renormalization parameters for the primary heat flows and determine the parameters by a linear least squares fit over the test period. Thus, the renormalized energy balance equation is

$$
\begin{aligned}
& Q_{int}(n) \\
+ p_o \cdot & \left[(L + L^{ch}_{infil}) \ (T_{in}(n) - T_{out}(n)) \right] \\
+ & \left[-L_b \ (T_{in}(n) - T_{bsm}(n)) \right] \\
+ p_{in} \cdot & \ Q^{in}_{storage}(n)
\end{aligned}
$$

$$+ \quad Q^{out}_{storage}(n)$$
$$+ \; p_{sun} \cdot Q_{sun}(n)$$
$$+ \quad [Q_{infil}(n) + L^{ch}_{infil} (T_{in}(n) - T_{out}(n)]$$
$$+ \quad Q_{sky}(n) \; , \qquad (4\text{-}2)$$

where p_o, p_{in}, and p_{sun} are the renormalization parameters. The problem is now reduced to determining these parameters. More generally, $Q^{in}_{storage}$ can be decomposed into two or more components, each with its own renormalization parameter. We will not consider those situations in this report. Also, Q_{sun} can have more than one parameter associated with it. This is considered later in this report.

The renormalized energy balance in Eq. 4-2 plays a central role in the PSTAR method.

4.2 Step 2: Audit Description

The explicit calculation of the heat flow terms of Step 1 is done in Section 4.5. We will simply note that this requires an audit description of the building. The flows $[-L\ (T_{in}(n) - T_{out}(n))]$ and $[-L_b\ (T_{in}(n) - T_{bsm}(n))]$ are directly obtained once L and L_b are known; L and L_b are computed from an audit description using the familiar UA summation. This obviously requires the wall layer thicknesses and conductivities, and the film coefficients. The flows $Q^{in}_{storage}(n)$, $Q^{out}_{storage}$ and Q_{sky} are calculated from a frequency response fitting procedure described in Subbarao (1988a). This also requires the thermal capacity of the materials as well as for the emissivities and orientations of various surfaces. These are required for Q_{sky}. The flow $Q_{sun}(n)$ is obtained, as noted before, from a microdynamic simulation of the audit building with $T_{in} = T_{out}$ = constant and with all other heat flows set to zero. The resulting cooling load gives Q_{sun}. A modified version of SUNCODE-PC (Palmiter and Wheeling 1982) was chosen as the microdynamic simulator; the modifications were done by Larry Palmiter. The Appendix gives the input file for SUNCODE-PC. The information necessary for the calculation of the other terms can be extracted from this input file.

4.3 Step 3: Test Protocol

The test data are needed to determine the three renormalization parameters: p_o, p_{in}, and p_{sun}. The tests should elicit these parameters. If one can arrange for the terms $Q^{in}_{storage}(n)$ and $Q_{sun}(n)$ to be small, it is clear from Eq. 4-2 that p_o can be determined. This is the idea behind coheating; by maintaining a constant indoor temperature for several hours through the night, the terms $Q^{in}_{storage}(n)$ and $Q_{sun}(n)$ can be made small during the last few hours. The last two hours of data were used in analysis. This 2-hr window elicits p_o. Having obtained p_o, a nighttime window with varying T_{in} (a cool down, for example) elicits p_{in}. Having obtained p_o and p_{in}, the daytime window elicits

p_{sun}. The tests, therefore, are done over about 36 hours in two nights (a night of coheating, a night of cool down) and the intervening day*.

For strongly solar-driven buildings, the daytime must be typically sunny. This may extend the duration of the tests. Heating or cooling system tests involve estimation of additional renormalization parameters and correspondingly require additional data.

The one-time tests are needed for obtaining infiltration heat flow. The common methods are tracer gas method or blower-door pressurization or depressurization method. While the tracer method measures infiltration directly, the blower-door method has the advantage of being inexpensive and is popular for leakage diagnosis. For this reason, the blower door method along with the Sherman-Grimsrud model (1980) was chosen.

In any case, it is clear that once the primary and secondary terms are identified, the renormalized energy balance equation guides one to a suitable test protocol. There are still experimental questions as well as questions on optimization of protocol. For example, for given electric heat input capacity and expected nighttime weather, how should one select the indoor temperature? How does one perform tests at different times of the year? One possible solution is to set the thermostat at the actual air temperature at, say, 7 p.m., instead of setting the thermostat at some value such as 70°F. This procedure generally results in a longer period of constant indoor temperature during the night. This improvement in the coheating tests evolved during discussions with C. Christensen and L. Palmiter.

Let us note in passing that if the term $[-L_b\ (T_{in}(n) - T_{bsm}(n))]$ were deemed to be a primary term, we would have an additional renormalization parameter, say, p_B, associated with this term. To elicit p_o and p_B simultaneously, we need two coheating periods (denoted by unprimed and primed values). If the determinant

$$\begin{vmatrix} (T_{in} - T_{out}) & (T_{in} - T_{bsm}) \\ (T_{in} - T_{out})' & (T_{in} - T_{bsm})' \end{vmatrix} \qquad (4\text{-}3)$$

is large enough, p_o and p_B are well-determined. Thus, two nights of coheating, arranged so that the determinant is large enough, should give a good determination of p_o and p_B. The test protocol consists of two nights of coheating, a

*Coheating tests were introduced by Sonderegger, Condon, and Modera (1980). Cool-down tests to assess the heat capacitance of a building were described by several authors. Duffy and Saunders (1987) developed a method that combines the loss coefficient from coheating, time constant from cool down, and measured window areas with a monthly correlation model or a simplified network model for long-term extrapolation. The PSTAR method uses the coheating and cool-down data along with daytime data to obtain a realistically complex model with a small number of parameters to be estimated. Solar dynamics are also obtained from using performance data. Additional tests, such as sinusoidal heat input tests are useful, but not necessary.

night of cool down, and daytime data on a relatively sunny day. A crude analysis of errors of estimation shows that it is generally difficult to get good values of p_o and p_B individually. One will then have to resort to setting p_B to unity, and estimating p_o. While only one coheating period would then be necessary, having two coheating periods is useful. See Section 4.6.

From the previous discussion, it is clear that the necessary data channels are:

- Indoor air temperature (weighted average of several representative indoor temperatures)
- Outdoor air temperature
- Crawl space air temperature
- Solar irradiance on at least two surfaces: global horizontal and at least one nonhorizontal, preferably vertical, on the primary orientation. This enables a measurement-based inference of ground reflectivity.
- Wind speed
- Electrical power.

A night of coheating, a night of cool down, and daytime data are needed. (Additional data with the heat pump operating were taken and will be reported separately.) A one-time blower door measurement is necessary.

4.4 Step 4: Test Data

The data channels consisted of:

- Indoor air temperature (weighted average of four temperatures)
- Outdoor air temperature
- Crawl space air temperature
- Solar irradiance (global horizontal as well as west vertical)
- Wind speed
- Electrical power (six circuits were monitored separately).

Figures 4-1 through 4-4 give plots of the data channels from March 15 to March 17, 1988.

The four interior temperatures are shown in Figure 4-1. It is apparent that there is typically a gradient of several degrees, related to where heaters are placed and solar gains. An area-weighted average temperature was used as the indoor temperature. A multizone formulation of PSTAR was discussed in Subbarao (1988a); it will be incorporated into future analysis.

The outdoor temperature and the crawl space temperature are shown in Figure 4-2. (The garage temperature, which was measured but not used except for qualitative purposes, is also shown in this figure.)

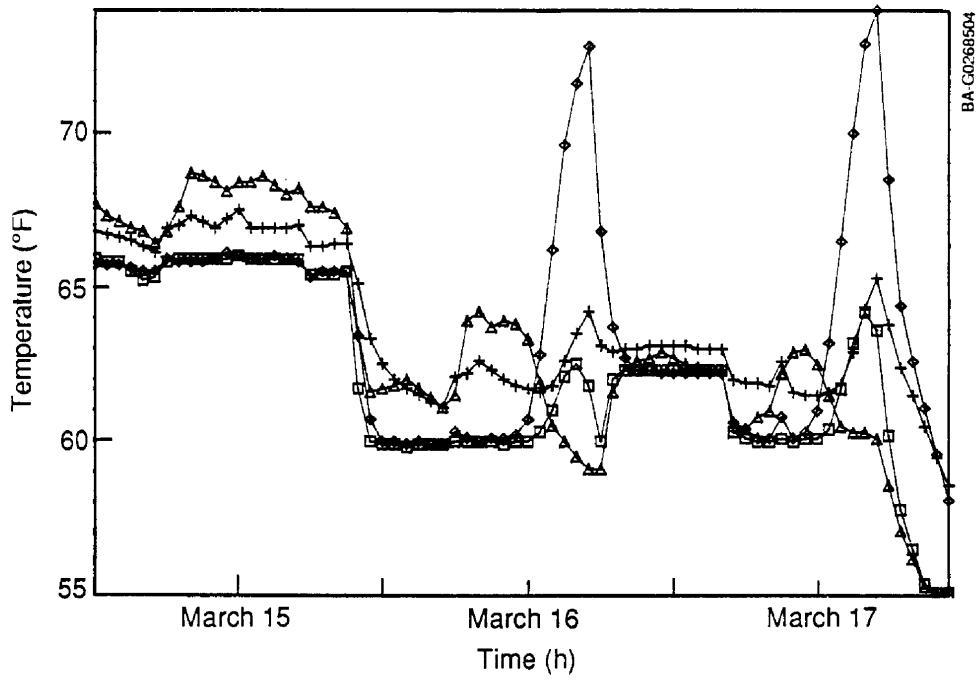

Figure 4-1. Hourly averages of indoor temperatures at several locations during the short-term tests held March 15-17, 1988. Coheating tests were performed during the first two nights and a cool-down test on the last night. Note the solar-driven temperature excursion in the west-facing master bedroom. The weighted average is given in Figure 4-9.

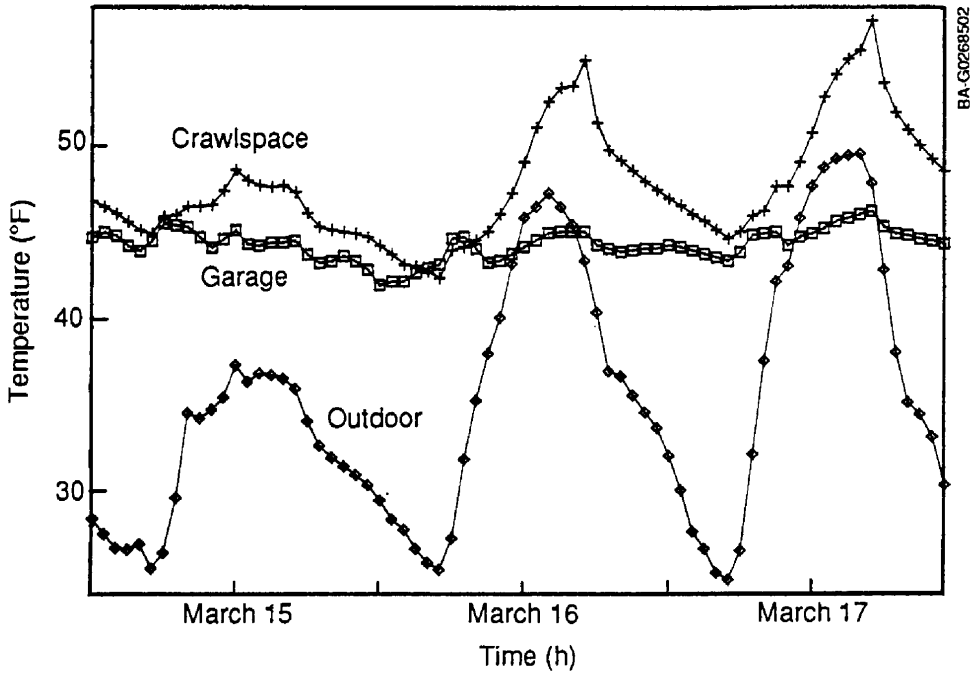

Figure 4-2. Hourly averages of outdoor, crawl space, and garage temperatures during the short-term tests

Figure 4-3 shows global horizontal irradiance as well as irradiance on the vertical westerly face of the building. The westerly orientation was chosen because the dominant solar gains into the building were deemed to be from this orientation. Figure 4-3 illustrates the wind speed. Electric power was separately monitored in six circuits (five had electric heaters, and one had the data acquisition system). Figure 4-4 shows the values.

4.5 Step 5: Calculation of Heat Flows

We now take up the calculation of each of the terms in Eq. 4-2. The plots of the various terms are arranged to avoid having an excessive number of plots.

1. $Q_{int}(n)$, the electrical power into the living zone, is the sum of powers in the six circuits of Figure 4-4, and is given in Figure 4-8.
2. From the audit description, the loss coefficient L is calculated through the familiar UA summation to be 473.1 Btu/hr°F. As discussed below, the average value of L_{inf}^{ch} was 385.3. With the measured values of T_{in} and T_{out}, the flow $858.4(T_{in}(n)-T_{out}(n))$ is easily calculated. For reasons we will clarify, 0.668 times this heat flow is shown in Figure 4-6.

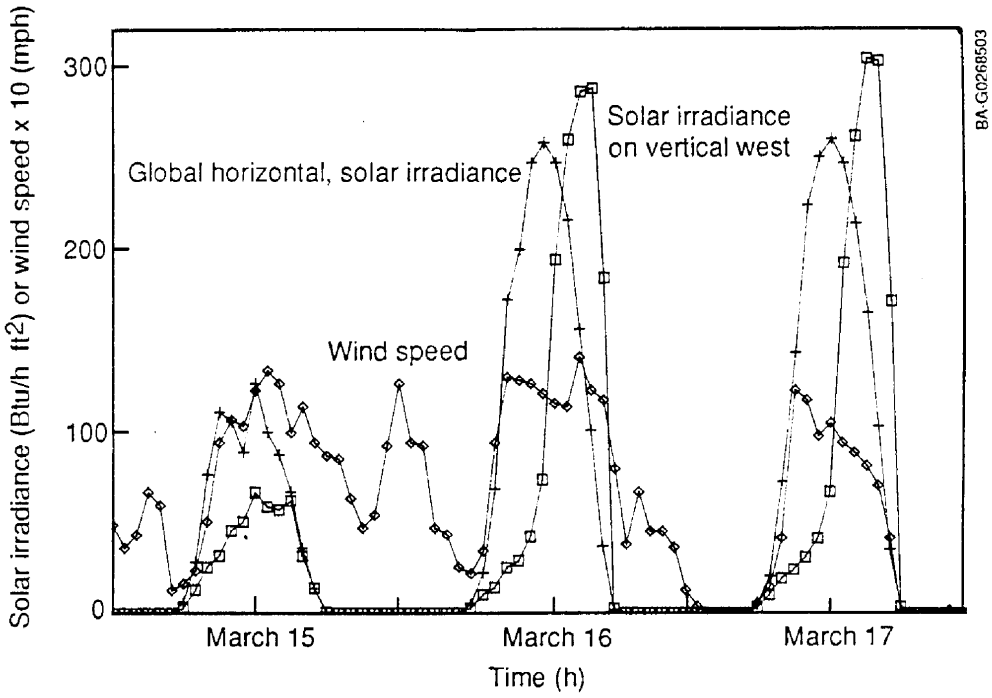

Figure 4-3. Hourly averages of solar irradiance on a horizontal pyranometer as well as that on a vertical pyranometer mounted parallel to the house in the westerly direction. Wind speed is also shown. Note the correlation between wind speed and solar irradiance.

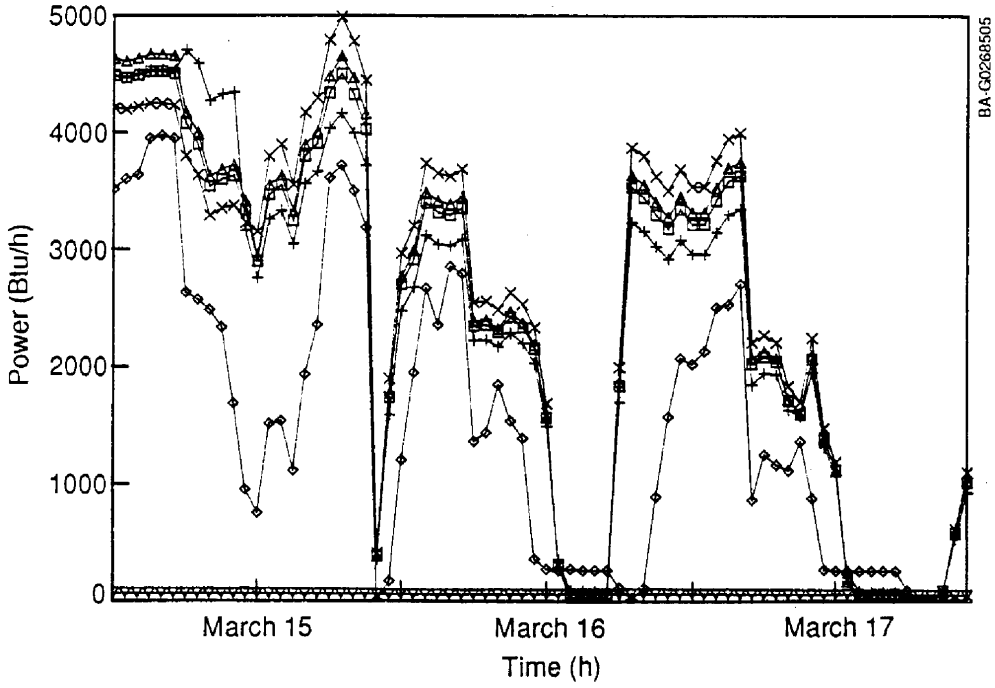

Figure 4-4. Hourly averages of power in the six circuits individually monitored. The total is plotted in Figure 4-8.

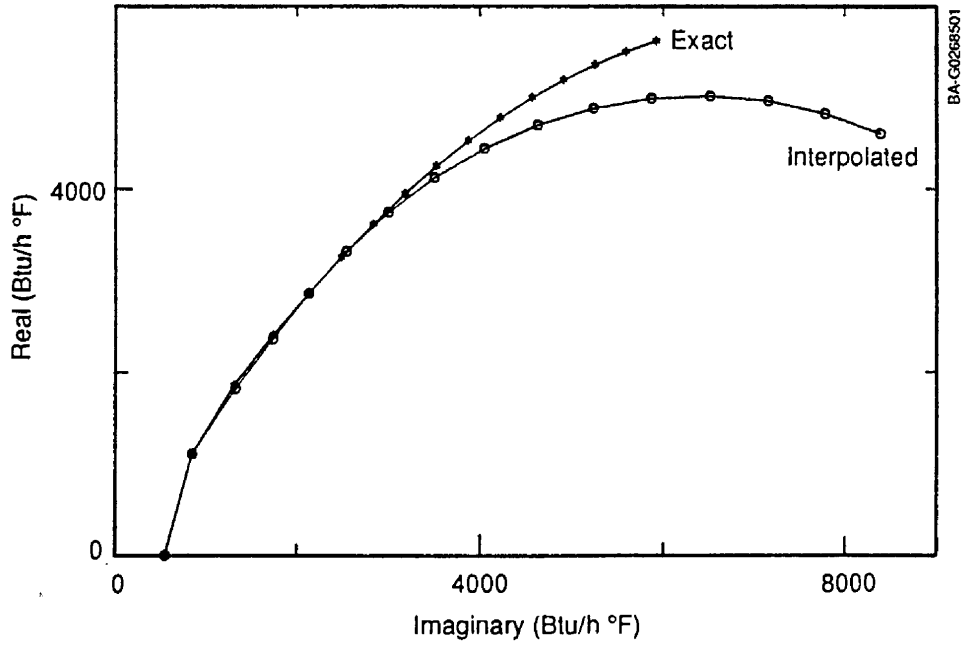

Figure 4-5. Polar diagram (imaginary vs. real part) of the V-admittance (i.e., admittance with respect to indoor temperature). The values based on the audit description are marked with an *, and those based on matching the audit building response at steady state, 48-hr, and 12-hr cycles are marked with an o. The n^{th} point on the curve (the first point being on the real axis) corresponds to a period of 48/(n-1). Thus the first, second, and fifth *'s and o's overlap.

3. From the audit description the coefficient L_b is calculated to be 75.7 Btu/hr°F. With the measured values of T_{in} and T_{bsm}, the flow $75.7(T_{in}(n)-T_{bsm}(n))$ is easily calculated and is shown in Figure 4-6.

4. The calculation of $Q^{in}_{storage}$ is quite involved and the method is detailed in Subbarao, 1988a. We will note here that the frequencies 0, $(48\ hr)^{-1}$, and $(12\ hr)^{-1}$ were chosen for response matching. Admittance (with respect to T_{in}) calculations from the audit description give 1389.8 (phase 52.58°) Btu/hr°F for the admittance at the 48-hr cycle and 3558.2 (phase 53.26°) Btu/hr°F for the admittance at the 12-hr cycle. The audit admittances as well as those based on matching at these frequencies are plotted in Figure 4-5. The latter are a good fit from low frequencies up to about the 8-hr cycle, and a reasonable fit for higher frequencies. We deem this

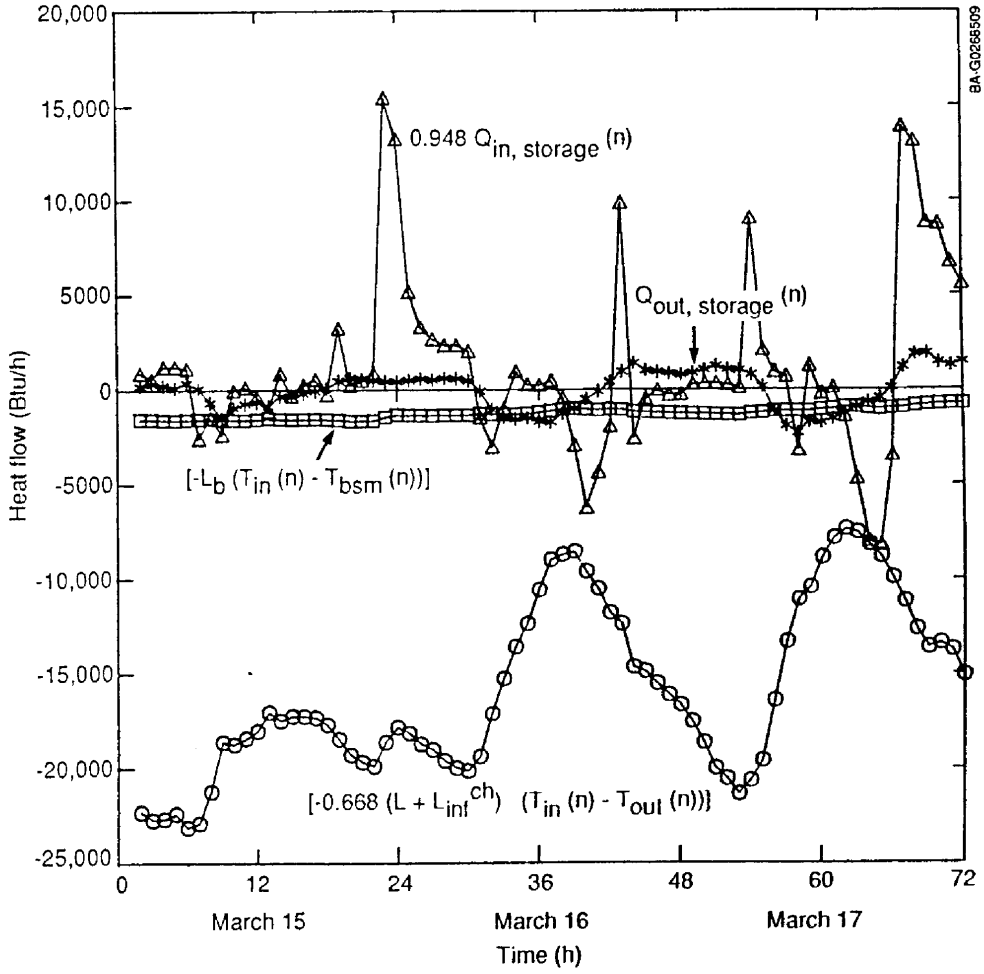

Figure 4-6. Plot of four of the heat flow terms: $[-0.668(L+L_{inf}^{ch})\cdot(T_{in}(n) - T_{out}(n))]$, $[-L_b\ (T_{in}(n) - T_{bsm}(n))]$, $0.948\ Q^{in}_{storage}(n)$ and $Q^{out}_{storage}(n)$. The renormalization factors are included in these plots (because the renormalized heat flows are the ones of interest). Positive values imply a heat gain by the air node and negative values a heat loss.

fit adequate and will proceed. The values of the α's are -0.00185 and 0.78429. These satisfy the stability criterion. The corresponding values of β are 4869.8 and 999.2 Btu/°F. From these values and the values of $T_{in}(n)$ (note that no other measurements are needed), one can calculate $Q^{in}_{storage}(n)$; for reasons that will become clearer, 0.948 times $Q^{in}_{storage}(n)$ (n) is shown in Figure 4-6.

5. The calculation of $Q^{out}_{storage}$ is similar to that of $Q^{in}_{storage}$. By fitting the admittance (with respect to T_{out}) at the 24-hr cycle, that was computed from the audit description to be 411.0 (phase -17.25°) Btu/hr°F, the following coefficients were obtained: $\alpha_1 = 0.6679$, $\beta_1 = -220.9$ Btu/°F. This satisfies the stability criterion. The fit is not especially good at higher frequencies, but because this is a secondary term, we will not attempt any further improvements. From these coefficients and the measured values of T_{out}, $Q^{out}_{storage}(n)$ can be calculated; the results are plotted in Figure 4-6.

6. The quantity Q_{sun}, the solar gain to the air node, was computed as the cooling load from the SUNCODE simulation with inside and outside temperatures as well as the crawl space temperature set to constant and equal values, and with internal gaines set to zero. For reasons that will become clear later, the resulting values, 0.895 times $Q_{sun}(n)$, are shown in Figure 4-7.

The calculations require values for ground reflectivity, normal beam irradiance I_{beam}, and for total global horizontal I_{ghor}. Ground reflectivity was derived from the vertical pyranometer, using the horizontal pyranometer reading as the basis for the correlation-based beam-diffuse split. Assuming an isotropic diffuse sky, it is easy to show that:

$$\text{Ground Reflectivity} = (I_{tot}(n) - I_{beam} \cdot \cos(i) - F_{sky} \cdot I_{dif,ghor}) / (F_{gr} \cdot I_{ghor}) \quad (4\text{-}4)$$

where: $I_{tot}(n)$ is the global total at orientation n
F is the view factor to sky or ground
i is the angle between n and the beam radiation.

The values of I_{beam} and I_{ghor} were obtained from a correlation between diffuse fraction and K_t defined to be the ratio $I_{dif,ghor}/I_{ghor,extraterrestrial}$ as derived in Erbs (1984).

The hourly values of ground reflectivity can be averaged over a day to obtain daily average values. Knowing the ground reflectivity, one can obtain values for I_{beam} and I_{ghor} from the vertical pyranometer readings. A weighted average of the values of I_{beam} (similarly I_{ghor}) based on the two pyranometers can now be obtained.

Any number of pyranometers, in any orientations, may be used to derive weighted average values. By assigning all the weight to one pyranometer (such as that pyranometer oriented the same as the house's dominate glazings), the beam-diffuse split can be based on that one pyranometer.

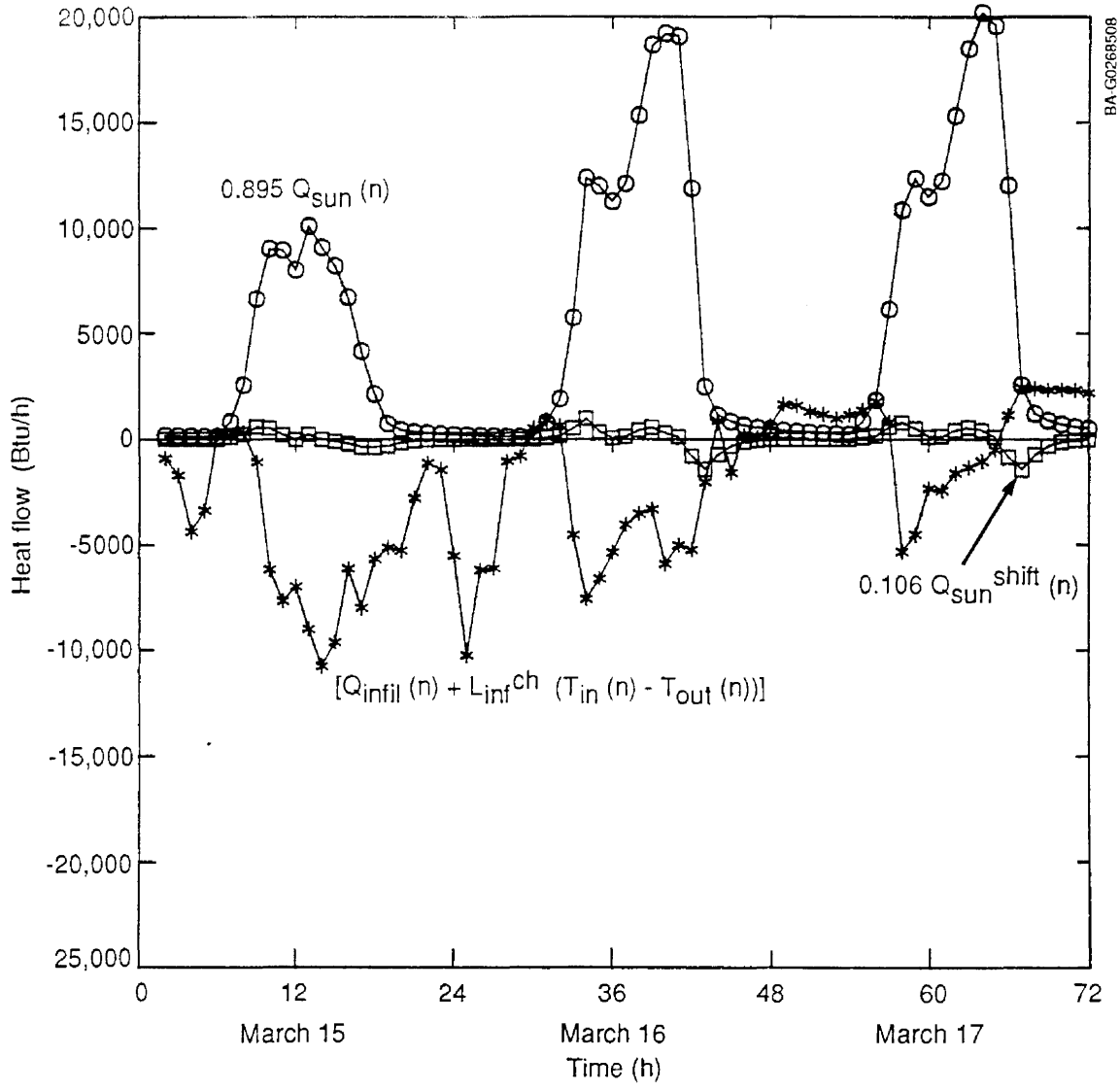

Figure 4-7. Plot of three of the heat flow terms: $0.895\ Q_{sun}(n)$, $0.106\ Q_{sun}^{shift}(n)$, and $[Q_{infil}(n) + L_{inf}^{ch} \cdot (T_{in}(n) - T_{out}(n))]$. Note that the second heat flow is small. Note the rather high degree of correlation between the first and last terms. Positive values imply a heat gain by the air node and negative values imply a heat loss.

Although the above method has been successful in several cases, because of the limitations of the then-version of the software, shading from tall trees surrounding parts of the building created problems. For this reason, only the horizontal pyranometer readings were used and the ground reflectivity was set at 0.3. Because the building is not strongly solar driven, this was deemed adequate. The discussion of using multiple pyranometers

is given here for completeness, and is necessary for strongly solar-driven buildings.

7. The term $Q_{infil}(n)$ was obtained as follows: first a blower door test was done resulting in an equivalent leakage area 285 in.^{2}. The infiltration air change per hr ACH is assumed to be of the form

$$ACH = [a \cdot |T_{in}-T_{out}| + b \cdot V_{wind}2]^{\frac{1}{2}} . \quad (4-5)$$

The values of a and b were 0.0221 and 0.0139, respectively, as appropriate for a two-story structure with shielding class 4, and terrain class 4. Eq. 4-5 was then used to predict the infiltration:

$$Q_{infil} = (0.018) \cdot ACH \cdot (House\ Volume) \cdot (T_{in}-T_{out}) . \quad (4-6)$$

The average infiltration during the tests according to the above formula was 1.28 air changes per hour. The average value of L_{inf}^{ch} during the coheating windows (spelled out later) was 385 Btu/hr°F. From this the term, $Q_{infil}(n) + L_{inf}^{ch} \cdot (T_{in}(n) - T_{out}(n))$ is easily obtained. The result is shown in Figure 4-7.

8. The term Q_{sky} arises from the fact that the effective sky temperature is lower than T_{out} because of the small values for the extinction coefficient for air at infrared wavelengths. The sky temperature was computed using the measured dewpoint temperature and periodically observed and interpolated cloud cover values, with the correlations derived in Martin and Berdahl (1984).

Net heat loss from the building caused by sky temperature depression can be calculated as the solar gain with $I_{beam} = 0$, and I_{ghor} given by

$$I_{ghor} = H_{rad} \cdot (T_{out} - T_{sky}) \quad (4-7)$$

where H_{rad} is the linearized radiation coupling
T_{sky} is the black body sky temperature giving equivalent radiant flux.

It is easy to show that for a black horizontal surface, this diffuse radiation is equivalent to the net sky infrared flux because of the sky temperature depression (i.e., $T_{out}-T_{sky}$). For vertical surfaces, it was assumed that the effective temperature difference was 0.7 times that for horizontal. Infrared radiation exchanged between building and the ground is ignored. All surfaces were assumed to have an emissivity of 0.9.

The calculation of $Q_{sky}(n)$ is perhaps best done by the frequency response matching technique, much like the $Q_{storage}^{in}(n)$ and the $Q_{storage}^{out}(n)$ terms, except that the driving function is a negative diffuse "solar" radiation. For historical reasons, this calculation was actually done using SUNCODE much like Q_{sun} calculation. For the glazing, the product of the extinction coefficient and the glazing layer width is made large to absorb all radiation on the outside surface.

The resulting Q_{sky} values are plotted in Figure 4-8.

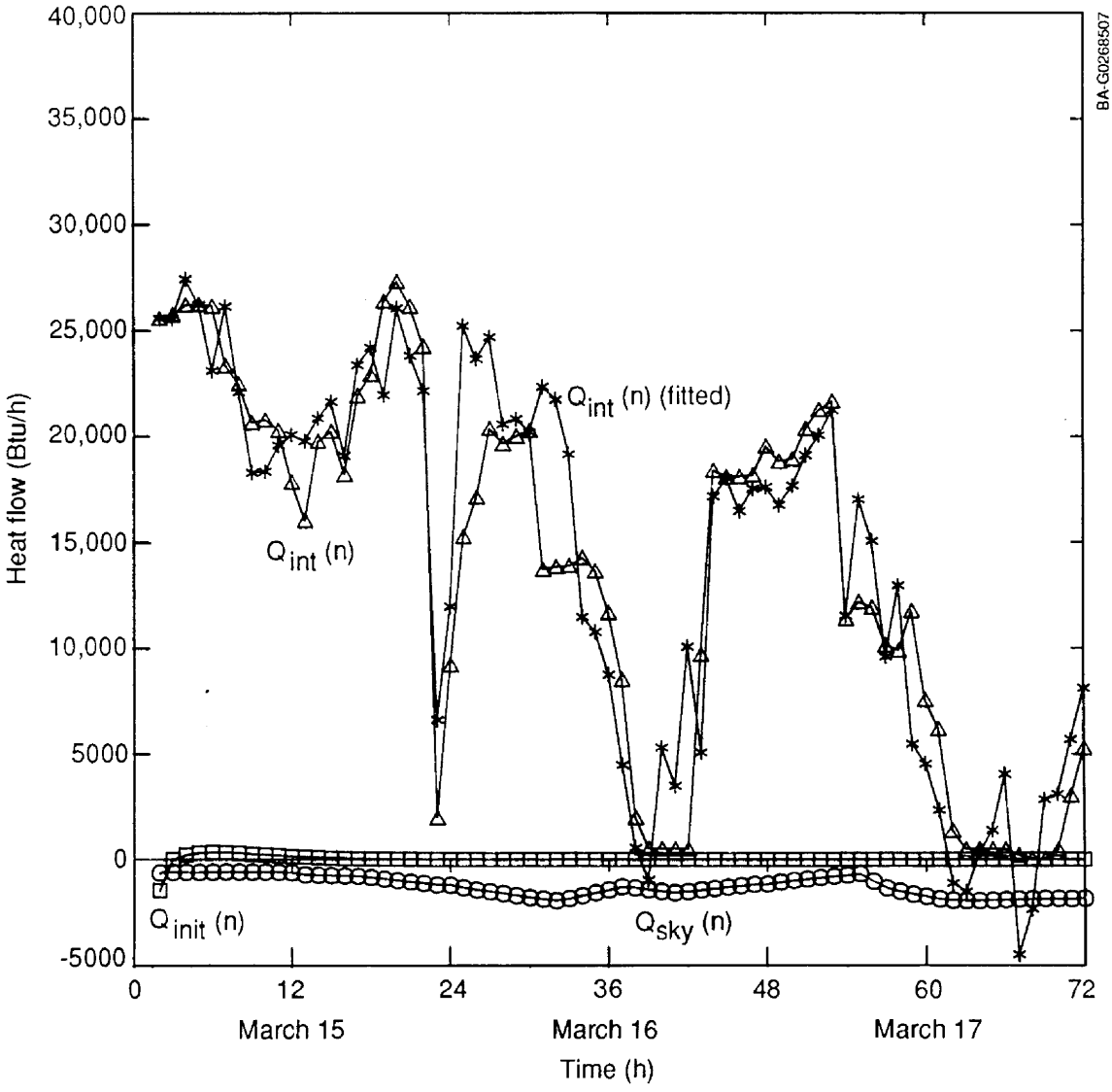

Figure 4-8. Plot of three of the heat flow terms: $Q_{int}(n)$, $Q_{sky}(n)$, and $Q_{init}(n)$. Note that the second is a secondary term. The last term decays exponentially, and is negligible after a few hours. Also plotted with an * are the best-fit values obtained for Q_{int} that were obtained from a least squares fit. The rms deviation between the measured and fit values is 3439 Btu.

4.6 Step 6: Renormalization of Heat Flows

The eight heat flow terms would add up to zero if the audit description matches the as-built building. Because this is unlikely, a renormalization of the primary heat flow terms is needed. Three renormalization factors p_o,p_{in}, and p_{sun} were introduced corresponding to the three primary terms. Additional parameters are introduced for the initialization as explained in Subbarao

(1988a); we will refer to these parameters collectively as (p_{init}). As we will see presently, these parameters can be avoided by allowing for a few hours of initialization.

The parameters are estimated sequentially and iteratively. Such a sequential and iterative procedure was introduced by Duffy (1987) in the context of an entirely different model.

The renormalization procedure is as follows: from the data, it can be seen that the final hours of the first coheating period are hours 28 and 29; the final hours of the second coheating period are hours 52 and 53. Two coheating periods were employed with a faint hope of extracting a renormalization factor for the L_b term also. Data analysis (as well as a simple error analysis) showed that this was not possible, and so the L_b term was treated as a secondary term. Two coheating periods were available, where only one would have been sufficient.

Iteration 1: start with $p_{in} = p_{sun} = 1$, and (p_{init}) set to zero. Use Eq. 4-2 during hours 28, 29, 52, and 53 to obtain p_o by linear least squares fit. With this value of p_o, use Eq. 4-2 during the hours 2 to 72 (one can exclude hours 28, 29, 52, and 53; this has a negligible effect) to obtain the rest of the parameters p_{in}, p_{sun}, and (p_{init}) using linear least squares fit.

Iteration 2: start with the improved values of the parameters p_{in}, p_{sun}, and (p_{init}). Use Eq. (4-2) during hours 28, 29, 52, and 53 to obtain improved value of p_o by linear least squares fit. With this improved value of p_o, use Eq. (4-2) during the hours 2 to 72 to obtain further improved values of the rest of the parameters p_{in}, p_{sun}, and (p_{init}), using linear least squares fit. Continue this sequential and iterative procedure until satisfactory convergence.

The iterations converged to a value of 0.667 for p_o, 0.914 for p_{in}, and 0.902 for p_{sun}. The root mean square deviation of the sum of heat flow terms from zero over the test period was 3453 Btu.

It follows that the conductance (including the average infiltration loss coefficient during the coheating periods) from the living zone to ambient is 572.3 Btu/hr°F. This should be compared with an audit value of 858.4. The audit value of 858.4 Btu/hr°F is made up of a skin loss coefficient of 473.4 and infiltration coefficient of 385.0 (this is the average value during the coheating hours given by the blower door model). The measured value of 572.3 can be disaggregated, if we take the infiltration coefficient of 385.0 seriously, into that value for infiltration and the remaining 187.3 Btu/hr°F for skin conductance. Although the audit skin loss coefficient of 473.4 is too high because of the use of rather high outside film conductances, and the use of a combined convection-radiation coefficient on the inside surfaces, we do not believe it should be as low as 187.3. We suspect that the infiltration value of 385 is too high because of inaccuracies in the blower door model of infiltration air flows as well as because of heat exchange effects in infiltration processes (Kohonen et al. 1985). The reason for introducing the L_{inf}^{ch} term in Eq. 4-2 is to evade the issue of how the value 572.3 is to be disaggregated into skin loss and infiltration loss. We believe the value of 572.3 as the measured total loss coefficient (skin conductance + average infiltration loss coefficient) is a reliable value. (One can introduce a

renormalization parameter for the $Q_{infil}(n) + L_{inf}^{ch} \cdot (T_{in}(n) - T_{out}(n))$ term and obtain it along with the other parameters. This gave a value of 0.74 with substantial error of estimation. The parameter p_o changed to 0.664, p_{in} to 0.878, and p_{sun} to 0.825; it can be qualitatively seen that solar radiation and wind were somewhat correlated during the test period.)

The parameter p_{in} was 0.914. This implies that the heat flow from charging and discharging of the masses because of indoor temperature fluctuations is 0.914 times that from the audit description. Roughly speaking, the building has less heat capacity than the audit description implies.

The parameter p_{sun} was 0.902. The solar gains are lower than the audit description implies. A number of effects, such as dirt on windows, window ledges, etc., presumably account for this factor.

A trend among several houses tested is for the loss coefficient to be less than the audit value, and for the solar gains also to be less than the audit value, whereas the parameter p_{in} is sometimes less than and sometimes higher than unity. The deviation of p_{sun} and p_{in} from unity is often higher than for this example building.

4.6.1. Inclusion of Solar Transfer Function

A simple multiplicative renormalization of $Q_{storage}^{in}(n)$ and $Q_{sun}(n)$ was used above. More complex schemes were discussed in Subbarao (1988a). Such schemes for $Q_{storage}^{in}(n)$ still result in a linear least squares estimate of parameters. They are rarely necessary for conventional buildings. We will not pursue them for this building. Although similar schemes are possible for $Q_{sun}(n)$ also, the need to deal with microsimulations in the Q_{sun} calculation makes such schemes cumbersome; a more manageable scheme was proposed in Subbarao (1988a) and will be implemented for our building. One of the motivations for having such a solar transfer function is that the audit description can be seriously wrong in regards to the distribution of solar radiation on different surfaces. For a weakly solar-driven building, such as our example, this is not really a major concern and we should not expect this transfer function to be significant. However, we will illustrate the scheme in the context of this building.

While the mathematical details are given in Subbarao (1988a), let us just note here that the "actual" solar gains Q_{sun}^{actual} are to be calculated from the audit gains Q_{sun} (in z-transformed space) as

$$p_{sun} \cdot Q_{sun} + p_{sun}' \cdot (1-z^{-1})/(1-\alpha_{sun} \cdot z^{-1}) \cdot Q_{sun} \; . \qquad (4\text{-}8)$$

In time domain, one can write

$$Q_{sun}^{actual}(n) = p_{sun} \cdot Q_{sun}(n) + p_{sun}' \cdot Q_{sun}^{shift}(n) \; , \qquad (4\text{-}9)$$

with the obvious definition of $Q_{sun}^{shift}(n)$.

The solar-related parameters to be estimated are p_{sun}, p_{sun}', and α_{sun} (in addition to the rest of the parameters). The parameter α_{sun} necessitates nonlinear least squares estimation. Fortunately, this can be reduced to a series of linear estimations. Since α_{sun} is constrained to be between 0 and 1, start

with, say, a value 0, and estimate all the other parameters and obtain the root mean square of the fit, Q(RMS). Change the value of α_{sun} to, say, 0.2 and re-estimate all the parameters and obtain Q(RMS). Vary α_{sun} over the range 0 to 1 and pick the value of α_{sun} and of the rest of the parameters, for which Q(RMS) is a minimum.

For our example, the results of such an analysis are shown in Table 4-1. The last row gives values for $p_{sun}' = 0$, which is the simple solar renormalization discussed earlier. We see there is a shallow, statistically insignificant minimum at α_{sun} equal to 0.4. The corresponding p_{sun}' is quite small; this indicates that the simple solar renormalization discussed earlier is very adequate. This can, in general, be caused by the building not being strongly solar driven, or the audit description for solar gains being generally correct except for transmittance.

The quantity $p_{sun}' \cdot Q_{sun}^{shift}(n)$ for $p_{sun}' = 0.106$ and $\alpha_{sun} = 0.4$ is shown in Figure 4-7. This is an extremely small heat flow.

The initial heat flow $Q_{init}(n)$ was estimated for the last run to be $-563860 \cdot (-0.00185)^n - 3181 \cdot (0.7843)^n + 4342 \cdot (0.6679)^n$. Figure 4-8 shows this term; it rapidly approaches zero as n increases.

Figure 4-8 presents internal gains computed from the renormalized energy balance equation.

The indoor temperatures predicted during the fitting period by the audit heat balance equation, by the renormalized heat balance equation, and the measured values are shown in Figure 4-9. There is a strong indication in the rapid decrease of the temperature of the audit building that the audit loss coefficient is too high. This was, of course, corrected by the renormalization process.

4.6.2 Simplified Renormalization

We will now discuss some simplifications possible in the renormalization process. we saw earlier that Q_{init} decays rapidly as a function of time. Suppose the heat flow terms are computed starting from hour 2. If the least squares estimation is performed over a period that begins several hours after hour 2, such as hour 7, then $Q_{init}(n)$ can be expected to be small from hour 7 onward and, hence, can be dropped. Unless otherwise warranted by the nature

Table 4-1. Goodness of Least Squares Fit for Different Values of α_{sun}

α_{sun}	p_o	p_{in}	p_{sun}	p_{sun}'	Q(RMS) Btu/hr
0.0	0.667	0.932	0.901	0.095	3446
0.2	0.668	0.941	0.899	0.110	3441
0.4	0.668	0.948	0.895	0.106	3439
0.6	0.668	0.948	0.891	0.081	3442
	0.667	0.914	0.902	0.000	3453

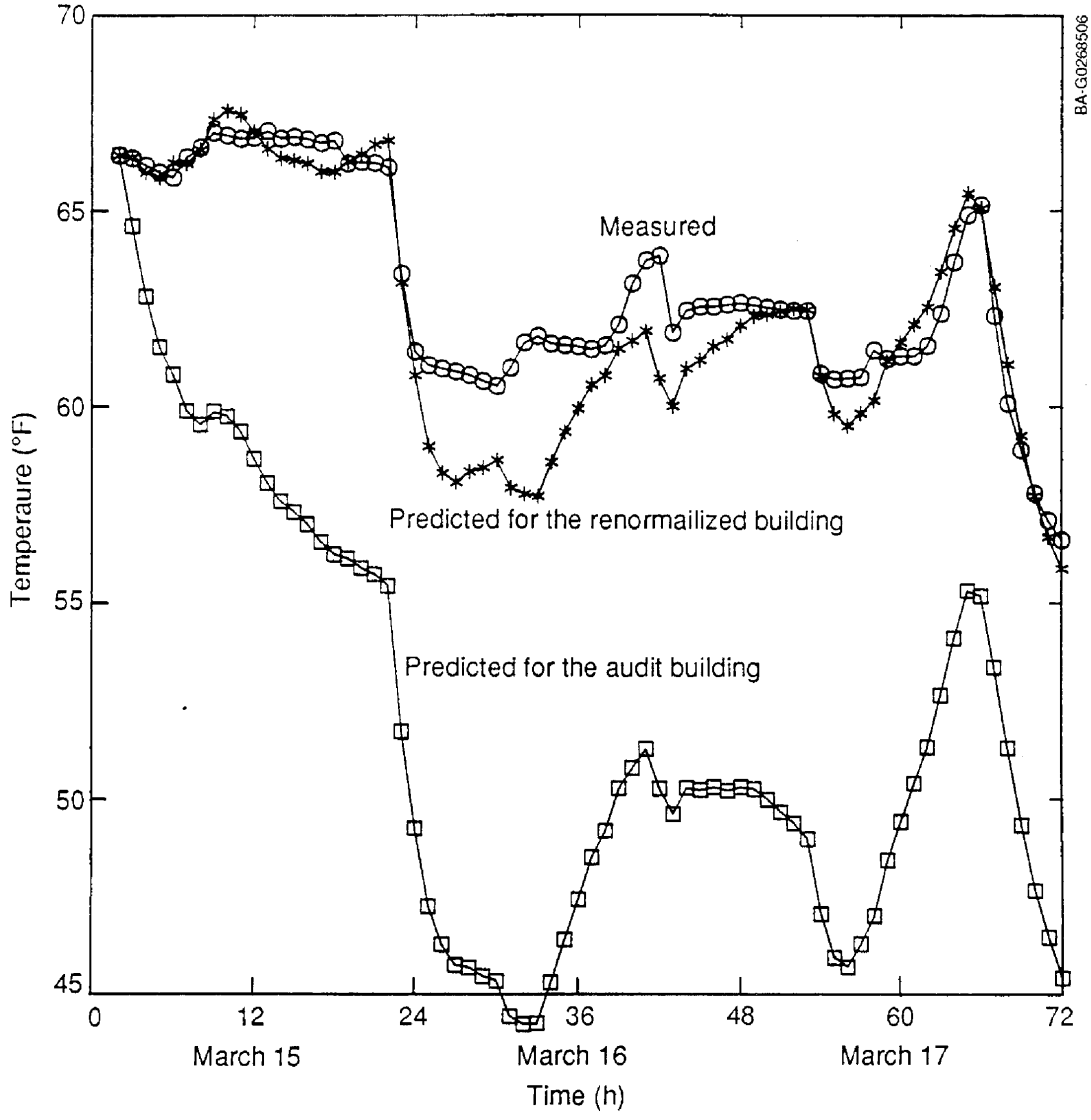

Figure 4-9. Plot of the measured indoor temperature, predicted by the audit (unrenormalized) energy balance equation, and predicted by the renormalized energy balance equation

of the building, we only use the simple multiplicative renormalization for solar gains. The heat balance equation then takes the form

$$
\begin{aligned}
& Q_{int}(n) \\
+ p_o \cdot & [-(L+L_{inf}{}^{ch}) \cdot (T_{in}(n) - T_{out}(n))] \\
+ & [-L_b\ (T_{in}(n) - T_{bsm}(n))] \\
+ p_{in} \cdot & Q^{in}_{storage}(n)
\end{aligned}
$$

$$+ \quad Q^{out}_{storage}(n)$$
$$+ \; p_{sun} \cdot \; Q_{sun}(n)$$
$$+ \quad [Q_{infil}(n) + L_{inf}{}^{ch.}(T_{in}(n) - T_{out}(n))]$$
$$+ \quad Q_{sky}(n) = 0 \; . \qquad (4\text{-}10)$$

In Section 4.5 we outlined the calculation of each one of the eight terms. The sequential and iterative procedure can now be used to determine the three parameters p_o, p_{in}, and p_{sun}.

Let us compute all heat flows starting from hour 2 as before. With the coheating windows chosen to be hours 28, 29, 52, and 53, as before, and with the window for p_{in} and p_{sun} chosen to be between hours 7 and 72, the following values were obtained: $p_o = 0.667$, $p_{in} = 0.915$, and $p_{sun} = 0.905$, with Q(RMS) = 3563 Btu/hr. These parameters are so close to the earlier ones that the accompanying simplifications are justified.

Thus, unless warranted otherwise by the nature of the building, this simplified renormalization procedure is recommended.

4.7 Step 7: Long-term Extrapolation

The renormalized energy balance equation can now be used to perform an hour-by-hour simulation of the as-built building. In particular, one can perform long-term extrapolation. Only the assumptions and results are given here. Details are given in Subbarao (1988a).

The extrapolation was done with the Washington typical meteorological year (TMY). The heating thermostat was set at 70°F from 7 a.m. to 11 p.m. with a setback to 60°F at other hours, and the cooling/venting thermostat set at 80°F. The crawl space temperature was assumed to be [60 + cos(2 · π(t-14)/24) + 5 cos(2 · π(t-5000)/ 8760)] °F corresponding to an average temperature of 60 with a diurnal amplitude of 1°F (peaking at 2 p.m.) and an annual amplitude of 5°F peaking in early August. (An alternative, and logically better approach, is to write an energy balance equation for the crawl space and proceed as we did for the living zone. While this is important for the evaluation of coupling of the crawl space to the ground, etc., its impact on long-term extrapolation is relatively minor. The simple method given here allows us to avoid dealing directly with ground-coupling issues.) The wind coefficient in infiltration calculation was suitably adjusted to account for the difference between TMY wind speeds and site wind speeds.

The simulation based on the renormalized energy balance gave the following results: (Corresponding values for the audit building, i.e., with unrenormalized energy balance, are given in parentheses.)

Annual Heating Load = 47.4 million Btu (79.8) (4-11)

Peak heating and cooling loads are also easily obtained. For example,

Peak Heating Load in January = 92.1 Kbtu/hr (109.2)
Peak Heating Load in February = 86.5 Kbtu/hr (103.3) (4-12)

Peak (sensible) cooling load in July = 22.4 Kbtu/hr (27.0)
Peak (sensible) cooling load in August = 24.1 Kbtu/hr (30.3) (4-13)

The annual heating load is significantly smaller than that for the audit building, primarily because of the difference in the loss coefficients. The difference is less pronounced in the peak heating loads because they are dominated by the morning start-up, and the effective capacitances of the audit and the renormalized buildings are not widely different (recall that p_{in} = 0.948 is close to unity). Peak (sensible) cooling loads are dominated by solar gains as well as indoor-outdoor temperature differences (recall that p_{sun} = 0.895).

Note that heating and cooling system efficiency should be considered in converting loads given below to energy consumption. This building has a heat pump; we plan to incorporate heat pump models in the near future.

In the previous calculations, we used SUNCODE to account for motion of the sun, shading, and angle of incidence modifications, diurnally as well as annually. Short-term tests that renormalize the calculated solar gains were performed over a few days in March. While the nonsolar related characteristics (such as the loss coefficient, charging, and discharging of masses due to inside and outside temperature variations) are expected to show no significant seasonal variations, the solar renormalization potentially may. This is because different components or orientations can dominate in different seasons. Thus, the use of the same renormalization of solar gains annually is suspect. This limits any short-term assessment of solar dynamics. It is desirable to have at least two determinations of solar dynamics: one in the heating season and one in the cooling season. Lacking two determinations, we used the solar renormalization from one short-term test over the entire year.

5.0 DISCUSSION

In this section we discuss some issues, efforts under way, and some open questions.

How does one determine which terms are primary and which are secondary? For most residential buildings $L(T_{in} - T_{out})$, $Q^{in}_{storage}$, and Q_{sun} are the three primary terms (excluding the space-conditioning system). The term $Q^{out}_{storage}$, for example, is secondary unless the building has uninsulated, massive exterior walls. If in doubt, we can treat $Q^{out}_{storage}$ as a primary term. The corresponding renormalization parameter will, very likely, be unreasonably far from unity. (Recall that, if the audit description is perfect, the renormalization parameters should be equal to one.) We expect the audit description to differ from the as-built description perhaps up to a factor of 2 or so, but not more. If a renormalization parameter is less than 0.5, or greater than 2.0, it signals a problem in the classification of terms into primary and secondary terms. (Large correlation between corresponding heat flow terms can also result in unreasonable values for the parameters.) One should, then, scrutinize the classification of terms and fix at unity the renormalization factor corresponding to the small terms; in other words, reclassify the term as secondary.

Given a transfer function formulation, it is easy to find a corresponding equivalent circuit (usually there is more than one). The circuit corresponding to the energy balance equation used for the building in this report (a two-frequency fit of the admittance with respect to inside temperature, a one-frequency fit of the admittance with respect to outside temperature, and a solar transfer function) can be derived.

The inside temperatures of buildings, in general, show spatial variations. A multizone formulation that takes this into account and rearranges the heat flows into primary and secondary terms was given in Subbarao (1988a); software incorporating this formulation needs to be developed and applied to the example building and other buildings.

A procedure to perform a basement (or crawl space) heat balance with primary and secondary terms and subsequent renormalization was outlined in Subbarao (1988a). It has no effect on the living zone energy balance and only a small effect on long-term extrapolation. Nevertheless, they need to be incorporated into the software.

The analysis reported here focused on the building alone and not on the HVAC system. During the short-term tests, the heat pump was operated on a third night. Analysis of these data require modeling the heat pump. Manufacturer's data provide a starting point (an audit description); it is then necessary to identify primary and secondary terms, and renormalize the primary term(s).

How good a representation of the as-built building heat balance is the renormalized energy balance? This is perhaps best answered through computer-generated data. A stripped-down example was given in Subbarao (1988a). A more systematic investigation is done by Palmiter, Toney, and Brown (1988); they concluded that the PSTAR approach shows considerable promise. Further investigations are needed.

The sensitivity of the renormalized energy balance to the initial audit description needs to be investigated.

An analysis of errors of estimation may appear to be straightforward because the estimation (at least in the absence of a solar transfer function) involves linear least squares. However, the sequential and iterative nature of the estimation requires further attention.

Are the parameter estimates repeatable? How accurate is the renormalized energy balance equation outside the test period? These questions need to be answered numerically as well as with real building tests. A test building at SERI is being monitored over several months. The analysis will be reported in the future.

The frequency response fitting procedure used here is generally adequate especially when high frequency behavior is not important. When it is, such as for peak loads, a method needs to be developed to provide a good fit over the entire range of frequencies of interest, satisfying the stability criterion, and preferably involving solution of only linear equations. High frequency response may have to be renormalized independently of the low frequency response.

What is the optimal protocol that elicits the maximum information with the least duration of the tests? How can one obtain the loss coefficient to the basement without large errors? These questions must be addressed.

6.0 SUMMARY AND CONCLUSIONS

PSTAR provides a unified method for building simulations and short-term tests. The various steps in the PSTAR process are:

- Identify all the relevant heat flows in the building contributing to the energy balance, disaggregated in terms of distinct driving functions. Classify the terms into primary, secondary, or measured terms.
- Obtain the audit description needed to calculate the flows.
- Determine a test protocol to elicit the renormalization parameters; the primary terms guide one in determining the protocol.
- Obtain test data.
- Calculate the heat flows for the test period. A macrodynamic method involving frequency response matching is employed in computing a number of the terms. A microdynamic simulator is used for computing solar gains.
- Obtain the renormalization parameters from linear least squares.
- Use the renormalized energy balance equation for the intended application.

Because only linear equations are encountered, the PSTAR method is mathematically reliable. Small heat flows, such as that due to sky temperature depression are all included. These steps were demonstrated for the Fredericksburg house.

The test protocol involves coheating, cool down, daytime data, and data with HVAC operation. Solar dynamics is obtained using daytime data. Sinusoidal heat input has the attractive feature of giving accurate values of the admittance with respect to indoor temperature, but are needed only for specialized applications, and are unnecessary for long-term extrapolation.

Annual heating and cooling loads as well as peak loads, with and without setback, can be obtained through hourly simulations based on the renormalized energy balance equation.

While long-term extrapolation is highlighted in this report, other important applications include HVAC diagnostics through building-as-a-calorimeter, predictive load control, and comparison of design versus actual thermal characteristics.

The synergism among macrodynamics (fitting admittances at selected frequencies and loss coefficients), microdynamics (solar gains), and short-term test data in giving quantitative as well as intuitive evaluation of a building has been demonstrated. Plots of the various heat flow terms contain a wealth of information in a compact form.

The PSTAR method forms the basis for the Short-Term Energy Monitoring (STEM) project at SERI. The goal of STEM is to assess the thermal quality of a residential building based on short-term tests during which a small number of data channels are measured. Setting up the instrumentation to measure a small number of data channels (approximately 20) typically takes less than half a person day. The tests last a few days. Analysis of the data provides extrapolation to long-term performance as well as important building parameters.

7.0. REFERENCES

Duffy, J.J., and D. Saunders, 1987. Low Cost Methods for Evaluation of Space Conditioning Efficiency of Existing Homes, Final Report to National Association of Home Builders (NAHB) Research Center, 400 Prince George Center Blvd., Upper Marlboro, MD 20772: NAHB Research Foundation, Inc.

Erbs, D., June 1984. Models and Applications for Weather Statistics Related to Building Heating and Cooling Loads, Ph.D. Thesis, Madison, WI: University of Wisconsin, Mechanical Engineering Department.

Kohonen, R., E. Kokko, T. Ojanen, and M. Virtanen, 1985. Thermal Effects of Air Flows in Building Structures, Research Report No. 367. Helsinki, Finland: Technical Research Centre of Finland.

Martin, M., and P. Berdahl, 1984. "Summary of Results from the Spectral and Angular Sky Radiation Measurement Program," Solar Energy Vol. 33, pp. 241.

Palmiter, L., and T. Wheeling, 1980. SERIRES 1.0, Golden, CO: Solar Energy Research Institute.

Palmiter, L., M. I. Toney, and I. Brown, 1988. Preliminary Evaluation of Two Short-Term Building Test Methods, Prepared for the Solar Energy Research Institute (SERI), under Contract No. HX-7-07146-1, Golden, CO: SERI.

Sherman, M.H., and D.T. Grimsrud, 1980. "Infiltration-Pressurization Correlation: Simple Physical Modeling," American Society of Heating, Refrigerating and Air Conditioning Engineers Transactions, Vol. 86, Part II.

Sonderegger, R., P. Condon, and M. Modera, 1980. "In Situ Measurement of Residential Energy Performance Using Electric Coheating," American Society of Heating, Refrigerating and Air Conditioning Engineers Transactions, Vol. 86, Part I, pp. 394.

Subbarao, K., 1988a. PSTAR - Primary and Secondary Terms Analysis and Renormalization: A Unified Approach to Building Energy Simulations and Short-Term Monitoring, SERI/TR-254-3175, Golden, CO: Solar Energy Research Institute.

Subbarao, K., 1988b. PSTAR - Primary and Secondary Terms Analysis and Renormalization: A Unified Approach to Building Energy Simulations and Short-Term Monitoring - A Summary, SERI/TR-254-3347, Golden, CO: Solar Energy Research Institute.

ATTCEILST	MAIN	1.63	<AREA>	ATTIC	1.63	<AREA>	159.0
FLOORCARPE	MAIN	1.3	<AREA>	CRAWLSPACE	1.3	<AREA>	1252.5
FLOORWOOD	MAIN	1.3	<AREA>	CRAWLSPACE	1.3	<AREA>	417.5
FLOORCAVI	MAIN	1.3	<AREA>	MAIN	1.63	<AREA>	1017.9
FLOORSTUD	MAIN	1.3	<AREA>	MAIN	1.63	<AREA>	152.6
ATTICROOF	ATTIC	1.63	<AREA>	ROOFEAST	4.	.8	779.4
ATTICROOF	ATTIC	1.63	<AREA>	ROOFWEST	4.	.8	485.0

SURFACES

* EXTERIOR SURFACE	COMPASS AZIMUTH [DEG]	TILT [DEG]	HEIGHT [FT]	LENGTH [FT]	OVERHANG TYPE	LEFT SIDEFIN	RIGHT SIDEFIN
*AAAAAAAAAA	XXX.X	XX.X	XXXX.XX	XXXX.XX	AAAAAAAAAA	AAAAAAAAAA	AAAAAAAAAA
NORTH1	0.	90.	10.	44.	EDGES	LNORTH	RNORTH
NORTH2	0.	90.	10.	44.	EDGES	<NONE>	<NONE>
WEST1	270.	90.	10.	24.	EDGESW1	<NONE>	<NONE>
WEST2	270.	90.	10.	24.	PORCH	<NONE>	<NONE>
WEST3	270.	90.	10.	24.	EDGESW3	<NONE>	<NONE>
SOUTH	180.	90.	10.	44.	EDGES	LSOUTH	RSOUTH
EAST1	90.	90.	10.	24.	EAVES	<NONE>	<NONE>
EAST2	90.	90.	10.	24.	EDGES	<NONE>	<NONE>
ROOFEAST	90.	30.	12.4	44.	<NONE>	<NONE>	<NONE>
ROOFWEST	270.	30.	12.4	44.	<NONE>	<NONE>	<NONE>

HVAC.TYPES

* HVAC TYPE	HEATING SETPOINT [F]	VENTING SETPOINT [F]	COOLING SETPOINT [F]	HEATING CAPACITY [KBTU/H]	VENTING CAPACITY [AC/H]	COOLING CAPACITY [KBTU/H]	COOLER COIL [F]
*AAAAAAAAAA	SSS.SSS	SSS.SSS	SSS.SSS	XXXX.XXX	XXX.XX	XXXX.XXX	XX.X
H1	68.	100.	68.	<ADEQ>	<ADEQ>	<ADEQ>	55.0
H2	68.	100.	68.	<ADEQ>	<ADEQ>	<ADEQ>	55.0

WALL.TYPES

* WALL TYPE	LAYER # 1	LAYER # 2	LAYER # 3	LAYER # 4	LAYER # 5	LAYER # 6
*AAAAAAAAAA	AAAAAAAAA	AAAAAAAAA	AAAAAAAAA	AAAAAAAAA	AAAAAAAAA	AAAAAAAAA
EXWALLCAVI	GYP.5	FIBBATT3	R-2.5	SIDING	<NONE>	<NONE>
EXWALLSTUD	GYP.5	STUD3.5	R-2.5	SIDING	<NONE>	<NONE>
CEILINCAVI	GYP.5	FIBBATT6	SIDING	<NONE>	<NONE>	<NONE>
CEILINSTUD	GYP.5	STUD6	SIDING	<NONE>	<NONE>	<NONE>
FLOORCARPE	CARPET	R-.1	WOOD.75	FIBBATT6	<NONE>	<NONE>
FLOORWOOD	OAK.75	WOOD.75	FIBBATT6	<NONE>	<NONE>	<NONE>
PARTITCAVI	GYP.5	R-1	GYP.5	<NONE>	<NONE>	<NONE>
PARTITSTUD	GYP.5	STUD3.5	GYP.5	<NONE>	<NONE>	<NONE>
HEAVYFURN	HEAVYFURN	R-20	<NONE>	<NONE>	<NONE>	<NONE>
FLOORCAVI	GYP.5	R-1	WOOD.75	OAK.75	<NONE>	<NONE>
FLOORSTUD	GYP.5	STUD10	WOOD.75	OAK.75	<NONE>	<NONE>
ATTICROOF	WOOD.75	SIDING	<NONE>	<NONE>	<NONE>	<NONE>
ATTCEILCA	GYP.5	FIBBATT10	<NONE>	<NONE>	<NONE>	<NONE>
ATTCEILST	GYP.5	STUD10	<NONE>	<NONE>	<NONE>	<NONE>

MASS.TYPES

*MASS TYPE	CONDUCTIVITY [BTU/FT-F-H]	DENSITY [LB/CF]	SPECIFIC HEAT [BTU/LB-F]	THICKNESS [FT]	NODES
*AAAAAAAAAA	X.XXXX	XXXX.XXX	X.XXXX	XX.XXXX	XX.
WOOD.75	.0667	32.	.33	.0625	1.
OAK.75	.102	47.	.57	.0625	1.
STUD3.5	.0667	32.	.33	.292	1.
STUD6	.0667	32.	.33	.5	1.
STUD10	.0667	32.	.33	.833	1.
HEAVYFURN	.12	80.	.3	.25	1.
LIGHTFURN	.1	40.	.3	.1667	1.
GYP.5	.093	50.	.2	.0417	
SIDING	.0667	32.	.33	.0313	

```
 FIBBATT3          .027          1.5          .2          .2917      0.
 FIBBATT10         .027          1.5          .2          .8333      0.
 FIBBATT6          .027          1.5          .2          .5         0.
 CARPET            .1           20.           .34         .123       0.
GLAZING.TYPES
* GLAZING     GLAZING    SHADING EXTINCTION  INDEX OF  THICKNESS  NUMBER
*  TYPE       U VALUE     COEF.     COEF.   REFRACTION OF LAYER      OF
*          [BTU/SF-F-H] [FRAC]    [1/IN]     [NONE]     [IN]      LAYERS
*AAAAAAAAAA  SS.SSSSS  SS.SSSSS  X.XXXX     X.XXXX    X.XXXX      XX.
 DBLBUGSCR      .5         .6     0.5000     1.5260    0.1250       2.
 DBLBUGSCRE     .5         .4     0.5000     1.5260    0.1250       2.
 DBLCLEAR       .5         .9     0.5000     1.5260    0.1250       2.
 DBLCLEARW1     .5         .75    0.5000     1.5260    0.1250       2.
 DBLCLEARW3     .5         .78    0.5000     1.5260    0.1250       2.
OVERHANG.TYPES
* OVERHANG   VERTICAL  HORIZONTAL
*   TYPE      OFFSET   PROJECTION
*             [FT]       [FT]
*AAAAAAAAAA   XX.XX      XX.XX
 EDGES          0.         0.33
 EDGESW1        0.         0.6
 EDGESW3        0.         0.8
 PORCH          0.         7.0
 EAVES          0.         1.42
SIDEFIN.TYPES
* SIDEFIN     OFFSET   LENGTH OF
*  TYPE       TO SIDE  PROJECTION
*             [FT]       [FT]
*AAAAAAAAAA   XX.XX      XX.XX
 LSOUTH         2.         2.
 RSOUTH         2.         2.
 LNORTH         1.         1.33
 RNORTH         1.         1.33
OUTPUTS
* OUTPUT   TIME    UNITS   OUTPUT    BUILDING   OUTPUT    FORMAT?
*  TYPE   PERIOD           SEASON    ELEMENT    SECTION
*         [H/D/M] [E/M]                                    [Y/N]
*AAAAAAAA    A       A    AAAAAAAA     XXXX.      XXXX.      A
 ZONES       M       E    <ALL>           1.         5.      Y
 ZONES       M       E    <ALL>           1.         6.      Y
 ZONES       M       E    <ALL>           1.         1.      Y
 AMBIENT     M       E    <ALL>           1.         1.      Y
SCHEDULES
*SCHEDULE  SEASON  HR   VALUE    HR   VALUE    HR   VALUE    HR   VALUE
*AAAAAAAA AAAAAAAA XX. XXXX.XXX  XX. XXXX.XXX  XX. XXXX.XXX  XX. XXXX.XXX
 RHOGR     EDAY1     1.     .3
 RHOGR     EDAY2     1.     .3
 RHOGR     EDAY3     1.     .3
SEASONS
* SEASON      START DATE     STOP DATE     DAY OF WEEK
*  NAME         MON DAY       MON DAY    [ALL/M-F/S-S]
*AAAAAAAA       AAA XX.       AAA XX.          AAA
 EDAY1          MAR 15.       MAR 15.          ALL
 EDAY2          MAR 16.       MAR 16.          ALL
 EDAY3          MAR 17.       MAR 17           ALL
STATIONS
* STATION     LAT.  LONG.  ELEV.  FILENAME   DATA  UNITS  -START-  -STOP--
*  NAME     [DEG] [DEG]  [FT]              TYPE  [E/M]  MON DAY  MON DAY
*AAAAAAAAAA XX.XX XXX.X XXXXX. AAAAAAAAAA  XX.    A     AAA XX.  AAA XX.
 SITE       38.33  77.5   300. QSUNTMY       1.    M     MAR 15.  MAR 17.
```

Document Control Page	1. SERI Report No. SERI/TR-254-3356	2. NTIS Accession No.	3. Recipient's Accession No.

4. Title and Subtitle

Short-Term Energy Monitoring (STEM): Application of the PSTAR Method to a Residence in Fredericksburg, Virginia

5. Publication Date: September 1988

6.

7. Author(s) K. Subbarao, J.D. Burch, C.E. Hancock, A. Lekov, and J.D. Balcomb

8. Performing Organization Rept. No.

9. Performing Organization Name and Address

Solar Energy Research Institute
A Division of Midwest Research Institute
1617 Cole Boulevard
Golden, Colorado 80401-3393

10. Project/Task/Work Unit No. SB811241

11. Contract (C) or Grant (G) No.

(C)

(G)

12. Sponsoring Organization Name and Address

13. Type of Report & Period Covered: Technical Report

14.

15. Supplementary Notes

16. Abstract (Limit: 200 words)

This report describes a project to assess the thermal quality of a residential building based on short-term tests during which a small number of data channels are measured. The project is called Short-Term Energy Monitoring (STEM). Analysis of the data provides extrapolation to long-term performance.

The test protocol and analysis are based on a unified method for building simulations and short-term testing called Primary and Secondary Terms Analysis and Renormalization (PATAR). In the PSTAR method, renormalized parameters are introduced for the primary terms such that the renormalized energy balance is best satisfied in the least squares sense; hence, the name PSTAR. The mathematical formulation of PSTAR is detailed in earlier reports. This report describes the short-term tests and data analysis performed using the PSTAR method on a residential building in Fredericksburg Virginia.

The results demonstrate the ability of the PSTAR method to provide a realistically complex thermal model of a building, and determine from short-term tests the statics as well as the dynamics of a building, including solar dynamics.

17. Document Analysis

a. Descriptors: Residential Buildings, Solar Architecture, Space HVAC Systems, Passive Solar Heating Systems, Mathematical Models, Thermal Analysis

b. Identifiers/Open-Ended Terms

c. UC Categories: 232

18. Availability Statement

National Technical Information Service
U.S. Department of Commerce
5285 Port Royal Road
Springfield, Virginia 22161

19. No. of Pages: 43

20. Price: A03